ABSOLUTE MEASUREMENTS OF NITRIC ACID BY KILOMETER PATHLENGTH FT-IR SPECTROSCOPY AND THEIR INTERCOMPARISON WITH OTHER MEASUREMENT METHODS

Final Report

Contract No. A5-051-32

California Air Resources Board

May 1986

Co-Principal Investigators

Dr. Arthur M. Winer
Dr. Ernesto C. Tuazon

Program Research Staff

Dr. Heinz W. Biermann
Dr. Timothy J. Wallington

Statewide Air Pollution Research Center
University of California
Riverside, CA 92521

ARB-86:intercom

ABSTRACT

Measurements of ambient nitric acid (HNO_3) and ammonia (NH_3) concentrations were conducted using a Fourier transform infrared (FT-IR) spectrometer interfaced to an open-path, multiple-reflection optical system. These measurements provided benchmark data for gaseous HNO_3 and NH_3 during a field study, held at Claremont, California, September 11-19, 1985, which compared current analytical methods for determining nitrogenous species concentrations in the atmosphere. Signal averaging for ~5 minutes at a pathlength of 1150 meters and spectral resolution of 0.125 cm^{-1} afforded detection sensitivities of approximately 4 ppb for HNO_3 and 1.5 ppb for NH_3.

The most reliable FT-IR measurements of HNO_3 for comparison purposes were those obtained during September 14 and 17. Nitric acid concentrations were above the FT-IR detection limit most of the daytime hours during the smog episode of September 14 when O_3 peaked at >0.2 ppm; the highest HNO_3 concentration of 26 ppb was recorded at ~3:45 p.m.

The higher FT-IR detection sensitivity for NH_3 afforded a more precise and complete set of data than those obtained for HNO_3. Background NH_3 levels were generally 2-4 ppb but concentration "spikes" as high as 84 ppb were measured when the wind direction was from nearby agricultural sources. Hourly average concentrations of HNO_3 and NH_3 are reported, along with the calculated average concentrations for the sampling periods designated for the majority of the other measurement methods.

TABLE OF CONTENTS

		Page
Abstract		ii
Acknowledgments		iv
List of Figures		vi
List of Tables		vii
I.	PROJECT SUMMARY	I-1
II.	INTRODUCTION	II-1
	A. Statement of the Problem and Background	II-1
	B. Overview of Current Methods	II-2
III.	TECHNICAL APPROACH	III-1
	A. The Kilometer Pathlength FT-IR System	III-1
	B. Site Preparation and Transport of Equipment	III-4
	C. Sampling Schedule	III-4
	D. Operation of the Kilometer Pathlength FT-IR Spectrometer	III-6
	1. Optical Alignment	III-6
	2. Routine Monitoring	III-7
	E. Treatment of Data and Calibration	III-8
IV.	RESULTS AND DISCUSSION	IV-1
	A. FT-IR Measurements	IV-1
	B. DOAS Measurements	IV-12
V.	REFERENCES	V-1
VI.	APPENDICES	VI-1
	Appendix A: Hourly Average HNO_3 Concentrations (nanomoles m^{-3}) by Long Pathlength FT-IR Spectroscopy	VI-2
	Appendix B: Hourly Average NH_3 Concentrations (nanomoles m^{-3}) by Long Pathlength FT-IR Spectroscopy	VI-3
	Appendix C: Average HNO_3 Concentrations (nanomoles m^{-3}) by Long Pathlength FT-IR Spectroscopy for the Designated Sampling Periods	VI-4
	Appendix D: Average NH_3 Concentrations (nanomoles m^{-3}) by Long Pathlength FT-IR Spectroscopy for the Designated Sampling Periods	VI-5

ACKNOWLEDGMENTS

Stimulating discussion and valuable exchanges of technical information, for which we express our appreciation, took place at various times during this program with Drs. Douglas R. Lawson, John R. Holmes and Jack K. Suder, members of the California Air Resources Board research staff. We gratefully acknowledge Travis Dinoff, William D. Long, Ervin Mateer, and Phillip C. Pelzel for assistance in carrying out this research, and Christy LaClaire and Lucille Sanchez for typing this report.

This report was submitted in fulfillment of Contract No. A5-051-32 by the Statewide Air Pollution Center, University of California, Riverside, under the partial sponsorship of the California Air Resources Board. Work was completed as of April 15, 1986.

The statements and conclusions in this report are those of the contractor and not necessarily those of the California Air Resources Board. The mention of commercial products, their source or their use in connection with material reported herein is not to be construed as either an actual or implied endorsement of such products.

LIST OF FIGURES

Figure Number	Title	Page
II-1	Time-concentration profiles of ozone and other gaseous pollutants present in photochemical smog at Claremont, California, October 12-13, 1978	II-4
III-1	Schematic diagram of the longpath FT-IR and DOAS spectrometers	III-3
III-2	Layout of the field study site illustrating the positions of the longpath FT-IR and DOAS spectrometers relative to the instruments of the other participants	III-5
III-3	Single beam spectrum of ambient air at 1150 m pathlength and 0.125 cm^{-1} resolution	III-9
III-4	Reference spectra of gaseous HNO_3 (0.61 torr) and NH_3 (0.23 torr) at spectral resolution of 0.125 cm^{-1}, pathlength of 25 cm, total pressure with N_2 of 740 torr. The HNO_3 plot is offset by 0.30 absorbance (base 10) unit for clarity	III-10
III-5	Infrared absorption peaks of HNO_3 (lower trace) relative to atmospheric H_2O absorptions (upper trace) in the 870-910 cm^{-1} region	III-11
III-6	Infrared absorption peaks of NH_3 (lower trace) relative to atmospheric H_2O and CO_2 absorptions (upper trace) in the 1080-1120 cm^{-1} region	III-12
IV-1	FT-IR spectroscopic detection of HNO_3 during the pollution episode of September 14, 1985 in Claremont, CA. The arrows indicate the positions of the HNO_3 absorption peaks	IV-3
IV-2	FT-IR spectroscopic detection of NH_3 in Claremont, CA, on September 16, 1985. The arrow indicates the measurement peak of NH_3 at 1103.4 cm^{-1}	IV-11

LIST OF TABLES

Table Number	Title	Page
IV-1	Hourly Average HNO_3 Concentrations (ppb) by Long Pathlength FT-IR Spectroscopy	IV-2
IV-2	HNO_3 Concentration (ppb) vs. Time in Claremont, CA, on September 14, 1985 by Long Pathlength FT-IR Spectroscopy	IV-5
IV-3	HNO_3 Concentration (ppb) vs. Time in Claremont, CA, on September 17, 1985 by Long Pathlength FT-IR Spectroscopy	IV-6
IV-4	Average HNO_3 Concentrations (ppb) by Long Pathlength FT-IR Spectroscopy for the Designated Sampling Periods	IV-7
IV-5	Hourly Average NH_3 Concentrations (ppb) by Long Pathlength FT-IR Spectroscopy	IV-9
IV-6	Average NH_3 Concentrations (ppb) by Long Pathlength FT-IR Spectroscopy for the Designated Sampling Periods	IV-10
IV-7	Hourly Average NO_2 Concentrations (ppb) by Long Pathlength DOAS Spectroscopy	IV-13
IV-8	Hourly Average HONO Concentrations (ppb) by Long Pathlength DOAS Spectroscopy	IV-14
IV-9	Average NO_2 Concentrations (ppb) by Long Pathlength DOAS Spectroscopy for the Designated Sampling Periods	IV-16
IV-10	Average HONO Concentrations (ppb) by Long Pathlength DOAS Spectroscopy for the Designated Sampling Periods	IV-16

I. PROJECT SUMMARY

A newly assembled kilometer pathlength FT-IR spectrometer was operated by the Statewide Air Pollution Research Center (SAPRC) to provide absolute measurements of gaseous HNO_3 and NH_3 during the intercomparison study of nitrogen species methods which was sponsored by the California Air Resources Board (ARB). This field study was held at Claremont, CA in September 11-19, 1985 with participation by investigators from 19 research laboratories based in the United States, Canada and Italy. The longpath FT-IR method was one of only two spectroscopic techniques that were employed for the measurement of gaseous HNO_3. The SAPRC additionally operated its longpath differential optical absorption spectrometer (DOAS) system alongside the FT-IR system to provide supplementary data on HONO, NO_2, and the NO_3 radical.

The FT-IR instrumentation used in the present study consisted of a Sirius 100 spectrometer (Mattson Instruments, Inc.) equipped with a liquid N_2-cooled HgCdTe detector, fitted with external transfer optics, and interfaced to a 25-meter basepath, gold-coated, multiple-reflection optical system. Sampling was conducted by natural transport of air into the open optical path with spectral records being made of the air parcel at 2.4 meter above ground, the height of the system's optical axis. Routine monitoring consisted of ~5 minute scan averaging at 0.125 cm^{-1} resolution and a total pathlength of 1150 meters with four to five spectra being recorded per hour. Detection sensitivities for HNO_3 and NH_3 were approximately 4 ppb and 1.5 ppb, respectively.

Most of the field study period was characterized by low levels of pollution so that HNO_3 concentrations were totally below the FT-IR detection sensitivity for two days and only slightly above the detection limit for 2-4 hour durations during three other days. The most significant FT-IR data for comparison purposes for the remaining three days, when longer periods of detectable HNO_3 levels prevailed, were those recorded during the moderately severe smog episode of September 14 when O_3 levels peaked at >0.2 ppm and HNO_3 concentrations were above the FT-IR detection limit most of the daytime hours. A peak value of 26 ppb was recorded at ~3:45 p.m. and high hourly average HNO_3 concentrations of 21 and 19 ppb were measured during the hours 3-4 p.m. and 4-5 p.m., respectively. A

significant portion of the FT-IR data on some of the days was reported as upper limit values due to interferences to the spectra by intermittent (and untraceable) noise.

The higher FT-IR detection sensitivity for NH_3 afforded a more precise set of data than those obtained for HNO_3. Concentrations of 2-4 ppb were common background NH_3 levels in Claremont during the field study but very high instantaneous concentrations, such as the value of 84 ppb measured at 8:56 a.m. on September 16, occurred when winds from the south-southeast direction transported NH_3 from the agricultural areas of Chino and Ontario. Such wind conditions clearly occurred during the morning hours of September 16 and 17 and early afternoon of September 12 when maximum hourly average NH_3 concentrations of 33, 46 and 57 ppb, respectively, were measured.

The longpath DOAS measurements of HONO and NO_2 for the 8-day duration of the field study are reported here as supplemental data, although support for the operation of this spectrometer system originated from our other ARB field study (Contract No. A4-081-32). Although the NO_3 radical was one of the species intended for measurement by DOAS, its concentration was above the detection limit of 0.02 ppb only during a one-hour period around 8 p.m. each of the two days, September 13 and 14. The concentrations of NO_2 were always above the 4 ppb detection sensitivity, the hourly average varying from a minimum of 9 ppb recorded during the early afternoon hours of September 15 to a maximum of 135 ppb measured during the period 9-10 p.m. on September 12. Significant levels of HONO were observed from the late evening (~9 or 10 p.m.) to the early morning hours (up to 8 a.m.) with observed concentrations ranging from the 0.6 ppb detection limit to a maximum of 2.6 ppb around midnight of September 15/16.

Hourly average concentrations of HNO_3, NH_3, NO_2 and HONO are presented here, along with calculated average concentrations for specified sampling periods. However, no extended interpretation of the FT-IR and DOAS data, in the context of the results from other measurement techniques, is made in this final report. Such discussions will be more appropriate at a later date when the totality of data is made available by the project coordinators to all the individual participants of the intercomparison study.

II. INTRODUCTION

A. Statement of the Problem and Background

Reliable measurements of ambient levels of nitric acid (HNO_3), ammonia (NH_3), and aerosol nitrate levels, as well as nitrous acid (HONO) and the nitrate (NO_3) radical, are essential in elucidating the fates and impacts of oxides of nitrogen ($NO + NO_2 = NO_x$) emitted from mobile and stationary combustion sources. The gaseous and particulate species formed in the atmosphere from NO_x emissions are critically involved in photochemical air pollution, visibility degradation, acidic deposition and the formation of atmospheric mutagens. Thus in any large-scale airshed study of the kind proposed to begin in 1987 in the California South Coast Air Basin (CSCAB), it is important to have well-established and validated measurement methods for such species.

Unfortunately, the routine measurement of compounds such as HNO_3 (and species such as NH_3 and HONO), at part-per-billion concentrations in complex mixtures of primary and secondary pollutants, is not a straightforward matter (see Section B below). Indeed, research and development efforts to produce reliable monitoring instruments for gaseous HNO_3 have been under way for more than a decade. However, to date no single method has gained acceptance with respect to all the criteria of accuracy, sensitivity, convenience and cost effectiveness. For this reason, the California Air Resources Board (ARB) sponsored a multi-investigator intercomparison study, in September 1985, in which all current, viable measurement methods for nitric acid and particulate nitrate were evaluated and compared. Based on the results of this intercomparison study, it is expected that one or more methods will be selected for use in a multistation air monitoring network to be employed in the major airshed study scheduled to begin in the South Coast Air Basin in 1987.

The ARB invited Statewide Air Pollution Research Center (SAPRC) researchers to participate in the September 1985 intercomparison study with our kilometer pathlength Fourier transform infrared (FT-IR) and differential optical absorption spectrometer (DOAS) systems. At the time of ARB's invitation, these spectroscopic systems were committed to provide data on a host of key atmospheric constituents including HNO_3, HONO and the NO_3 radical in a summer field study at UCR under a separate ARB-sponsored program involving a coordinated study of the role of nitrogenous

pollutants in acid deposition and in the formation of atmospheric mutagens (Contract No. A4-081-32). The latter study was scheduled for the summer of 1985. This study was postponed by mutual agreement with the ARB partly due to the lack of elevated pollution levels through the end of July 1985 at our UCR site, but more importantly because of the necessity of having our long-path spectrometer set up in time for participation in the intercomparison study at Claremont in mid-September 1985.

Thus, SAPRC's specific role in the ARB-sponsored intercomparison study was to provide absolute measurements of gaseous nitric acid and ammonia by kilometer pathlength FT-IR spectroscopy. Our additional long path DOAS measurements provided supplementary data for NO_2, HONO and the NO_3 radical. Our spectroscopic HONO data, in particular, are important in testing the capability of relative methods such as filter packs and difference denuders for measuring this important species, or alternatively the extent to which HONO may constitute an interference in any of the HNO_3 and nitrate measurement methods employed in the intercomparison study. We note that although for completeness the nitrous acid data obtained in the Claremont study by our long path DOAS method are reported here, support for these measurements came from our other ARB sponsored research program (Contract No. A4-081-32) concerning field measurements of atmospheric species.

B. Overview of Current Methods

Available candidate methods for both gaseous nitric acid and particulate nitrates include a variety of filter and denuder tube arrangements which have been described in the literature (Stevens 1979, Fellin et al. 1980, Appel et al. 1981, Forrest et al. 1982, Shaw et al. 1982, Spicer et al. 1982, Gailey et al. 1983, Golden et al. 1983, Anlauf et al. 1984). Recently, Braman et al. (1982) and McClenny et al. (1982) have utilized a tungstic acid method for HNO_3, particulate ammonium and gaseous ammonia (NH_3). None of these methods provide absolute concentrations of, for example, HNO_3. They must therefore be calibrated against standard mixtures or absolute reference methods.

One recently developed absolute method is the tunable diode laser absorption system assembled by Schiff and his co-workers (1983). This

system was employed in a recent intercomparison study conducted under field conditions in southwestern Ontario, Canada. A tungstic acid denuder tube and a filter pack containing a Teflon/nylon/W41 filter combination were operated simultaneously, and their results for HNO_3 compared to those obtained with the tunable diode laser system (Anlauf et al. 1985). During this study, significant differences were observed at various times between the laser, filter pack and tungstic acid methods. Specifically, at night the tungstic acid method generally yielded larger concentrations (by about a factor of two) than the filter pack method, and at the peak HNO_3 concentration the laser values were more than a factor of two greater than either of the other two methods.

The SAPRC has, for the past 10 years, conducted periodic measurements of HNO_3 and NH_3 in ambient air in the CSCAB (Tuazon et al. 1978, Doyle et al. 1979, Tuazon et al. 1980, 1981). We have employed FT-IR spectrometers interfaced to multiple reflection systems capable of total optical paths of 1-1.5 km. For example, in a 1976 study at Riverside, we employed an eight-mirror optical cell originally developed by Hanst (1971) to make the first spectroscopic identification and measurement of HNO_3 (and of formaldehyde) in the troposphere (Tuazon et al. 1978). Measurements of HNO_3, and other species such as O_3, NH_3, PAN, HCHO and HCOOH, were subsequently made with this system at Claremont, a mid-basin site (Tuazon et al. 1981), and in east Los Angeles, a source area (Hanst et al. 1984). An example of the capability of kilometer pathlength FT-IR spectroscopy for absolute determinations of HNO_3 at concentrations above ~5 ppb, simultaneously with the other pollutant species and with good time resolution, is shown in Figure II-1. These data were obtained at Claremont during a severe photochemical air pollution episode in 1978.

The long-path infrared absorption method has, therefore, a successful record of providing absolute and specific concentrations for HNO_3 in complex pollutant mixtures. Although a lower detection limit is highly desirable for this technique, it is still clearly one choice for a reference method, particularly for levels of nitric acid typically encountered in moderate to severe smog episodes in the South Coast Air Basin. Our previous kilometer pathlength FT-IR system had, in fact, already played the role of a reference method during an EPA-sponsored field study in Claremont, CA, in August 27-September 3, 1979 (Spicer et al. 1982).

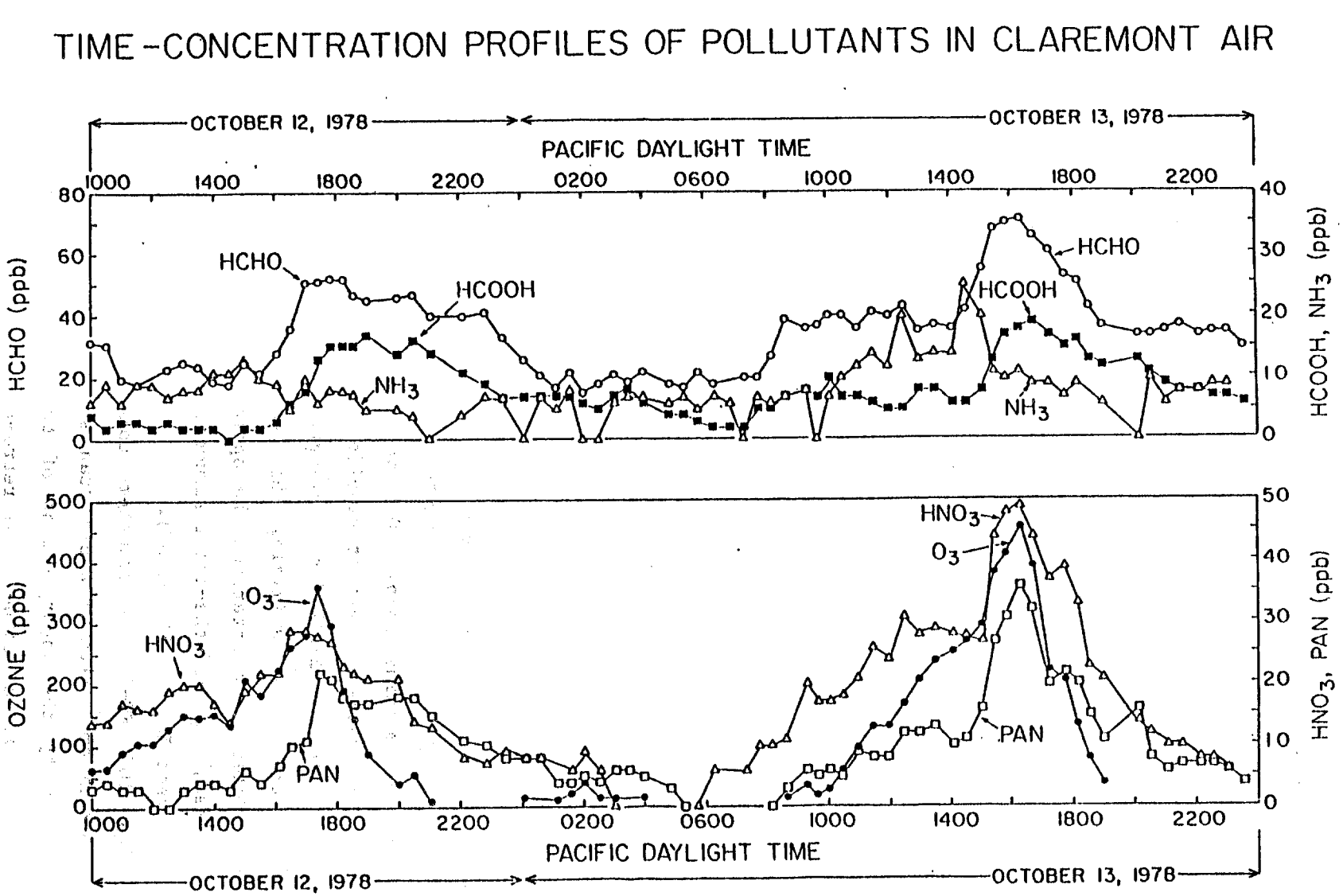

Figure II-1. Time-concentration profiles of ozone and other gaseous pollutants present in photochemical smog at Claremont, California, October 12-13, 1978.

III. TECHNICAL APPROACH

A. The Kilometer Pathlength FT-IR System

The SAPRC's present capability in infrared spectroscopic measurement of ambient air pollutants is based on a newly constructed 25-m basepath, open multiple-reflection optical system which can be interfaced to any of three FT-IR spectrometers available at the Center. The long-path optics is basically of the three-mirror White design (White 1942), but with an added corner reflector at the in-focus end, a modification due to Horn and Pimentel (1971), which effectively doubles the system's pathlength.

The mirrors in this new optical system were ground and polished from 30 cm diameter, 6 cm thick Pyrex blanks by Brunache Instrument Optics (Carlsbad, CA) and gold-coated for the best reflectivity (~99%) in the infrared by Keim Precision Mirrors Inc. (Burbank, CA). The optimum pathlength for monitoring was determined to be in the 1-1.5 km range during actual operation, although short-term use of optical paths greater than 2 km are possible.

We chose a kinematic mounting system which employs a design in which the weight of the mirror is totally supported by its central pivot. The latter consists of a socket attached to the center of the mirror backing plate, which rests and pivots on a ball end whose stem is secured to the support frame. The orthogonal adjustments are provided by micrometer screws which track on V-grooves and work against the positive action of a single compression spring. These mounts were fabricated by the UCR Chemistry Department machine shop. Our previous experience with this mirror mount design indicates that it provides alignment stability within temperature fluctuations of ±20°F for pathlengths of ~1000 meters.

With the objective of maximizing the capability of the long-path FT-IR system, we elected to interface the optical system described above to a newly acquired, state-of-the-art instrument: the Sirius 100 produced by Mattson Instrument Inc. (Madison, WI).

The Sirius 100 FT-IR spectrometer combines maximum resolution capability of 0.125 cm^{-1} with enhanced scan stability. The latter has been made possible by the incorporation of two design features in the interferometer: the use of corner cube retro-reflectors in place of the conventional plane mirrors, and the use of laser quadrature detection to

give an exact trigger point for each scan instead of the less stable and less accurate white light indexing of older interferometers.

The Sirius 100 is equipped with the 32-bit word Starlab computer which employs a UNIX operating system. The data system utilizes three Motorola 68000 and one Texas Instrument 9900 microprocessors and, in the present configuration, has 1 MB of main memory and 40 MB fixed disk storage with backup storage on diskette or magnetic tape. These features allow spectroscopic monitoring of ambient air to be carried out at a time resolution of up to five spectra per hour and with the enhanced sensitivity and information content afforded by high spectral resolution ($\sim$0.1 cm^{-1}).

The Sirius 100 instrument was housed in a backyard-type, air-conditioned shed adjacent to the kilometer pathlength optical system. The general optical layout is similar to that of our earlier configuration (Tuazon et al. 1978, 1980), except for the use of the more elegant White-Horn-Pimentel optics in an open cell, in place of the Teflon-enclosed, eight-mirror Hanst cell.

As has been indicated earlier, the long-path FT-IR spectrometer was operated alongside the long-path DOAS spectrometer in a unique combination of these two powerful, complementary techniques for the characterization of trace nitrogenous species in the atmosphere. The DOAS system in fact has the same design for the multiple reflection optics as the FT-IR system, except for the use of multilayer dielectric coatings on the mirrors. These coatings provided very high reflectivity in the UV-visible region of interest.

A diagrammatic representation of the two long-path spectrometers is given in Figure III-1. In practice, the arrangement is more compact (see Figure III-2), with both folded-path mirror systems arrayed in opposite directions but aligned side by side such that simultaneous analyses of virtually the same air sample is made. Design and operation of the DOAS spectrometer has been described elsewhere (Platt et al. 1980, Platt and Perner 1983, Pitts et al. 1984).

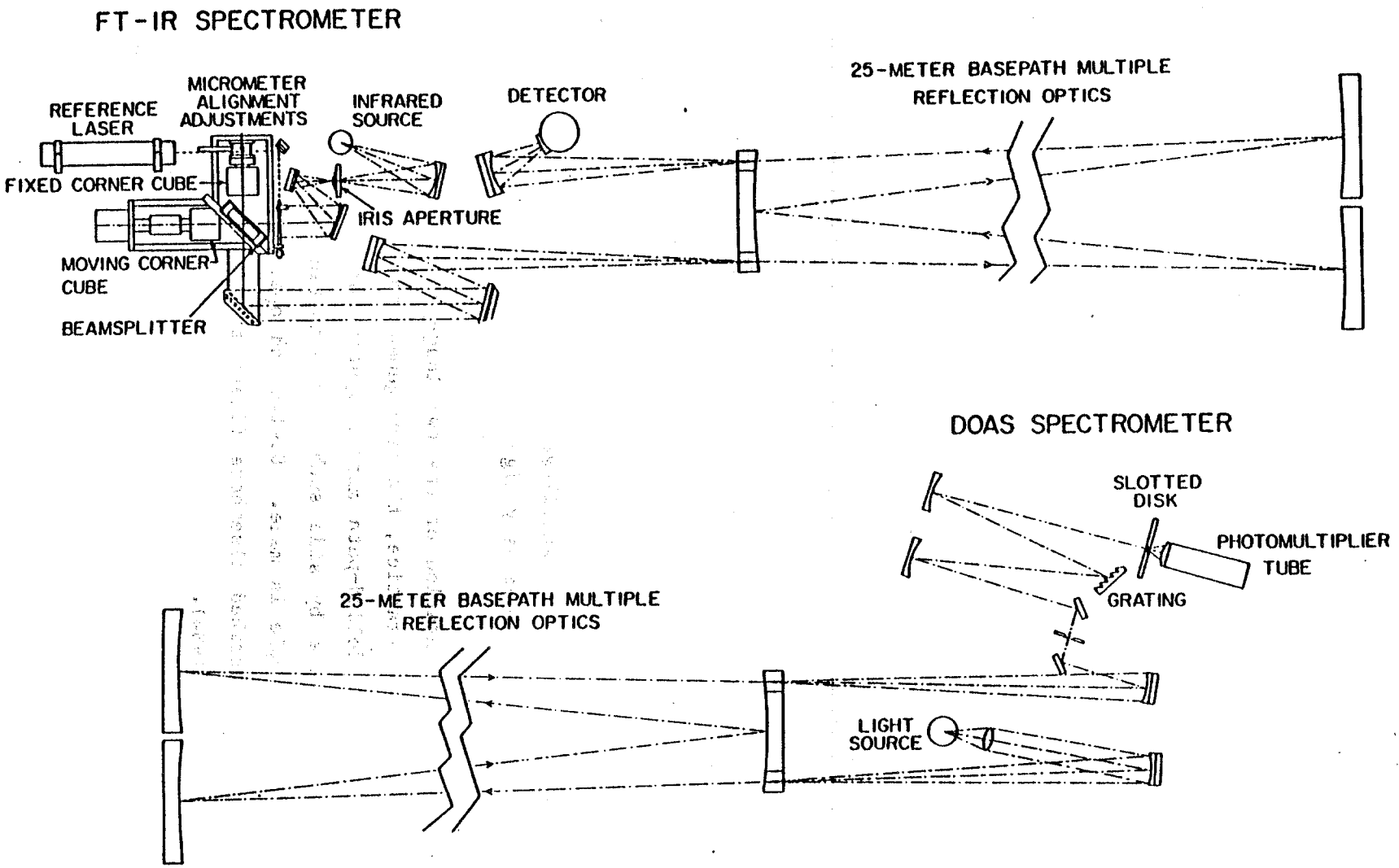

Figure III-1. Schematic diagram of the longpath FT-IR and DOAS spectrometers.

B. Site Preparation and Transport of Equipment

The site of the field study, which was chosen by the program coordinators, Drs. Douglas Lawson (ARB) and Susanne Hering (University of California, Los Angeles) was a parking lot on the east side of Pomona College in Claremont, CA. Vehicular activity around the site was restricted by the authorities at Pomona College such that primary emissions from automobiles did not cause interference problems for the duration of the study. A sketch of the layout of the sampling site is shown in Figure III-2 which illustrates the position of FT-IR and DOAS spectrometers relative to the instruments of other participants.

A critical requirement for the study was that all analytical techniques sample at a common height of 2.4 m (8 ft) above the ground in order to minimize influences of dry deposition of nitric acid. This requirement, however, introduced the major problem of restructuring our FT-IR and DOAS instrument support and housing. In order to provide the additional height needed to augment the 1.2 m height initially designed into the optical axes of both the FT-IR and DOAS long pathlength assemblies, and at the same time prevent extraneous vibrations, the spectrometers and mirror systems (and housings) were set on massive concrete blocks.

Six 4 ft x 4 ft x 8 ft concrete structures were rented from a local company which also provided the heavy machinery to position the blocks on premarked areas at the study site. Three each of these blocks constituted the support platform for the FT-IR and DOAS assemblies at each end of the sampling path (Figure III-2). New 9 ft x 12 ft sheds were procurred and constructed over these platforms during the last week of August and first week of September. Subsequent assembly and testing of the spectrometers and optical systems were completed in time for the scheduled start of the field study on September 11, 1985.

C. Sampling Schedule

A vast array of samplers for nitric acid and particulate nitrate which included such apparatus as filter packs, annular denuders, denuder difference set-ups, concentrators, as well as continuous monitors were brought into the study site by researchers from 19 participating laboratories. A sampling schedule was carefully designed to ensure good statistics taking into account such factors as sampling duration, side-by-side

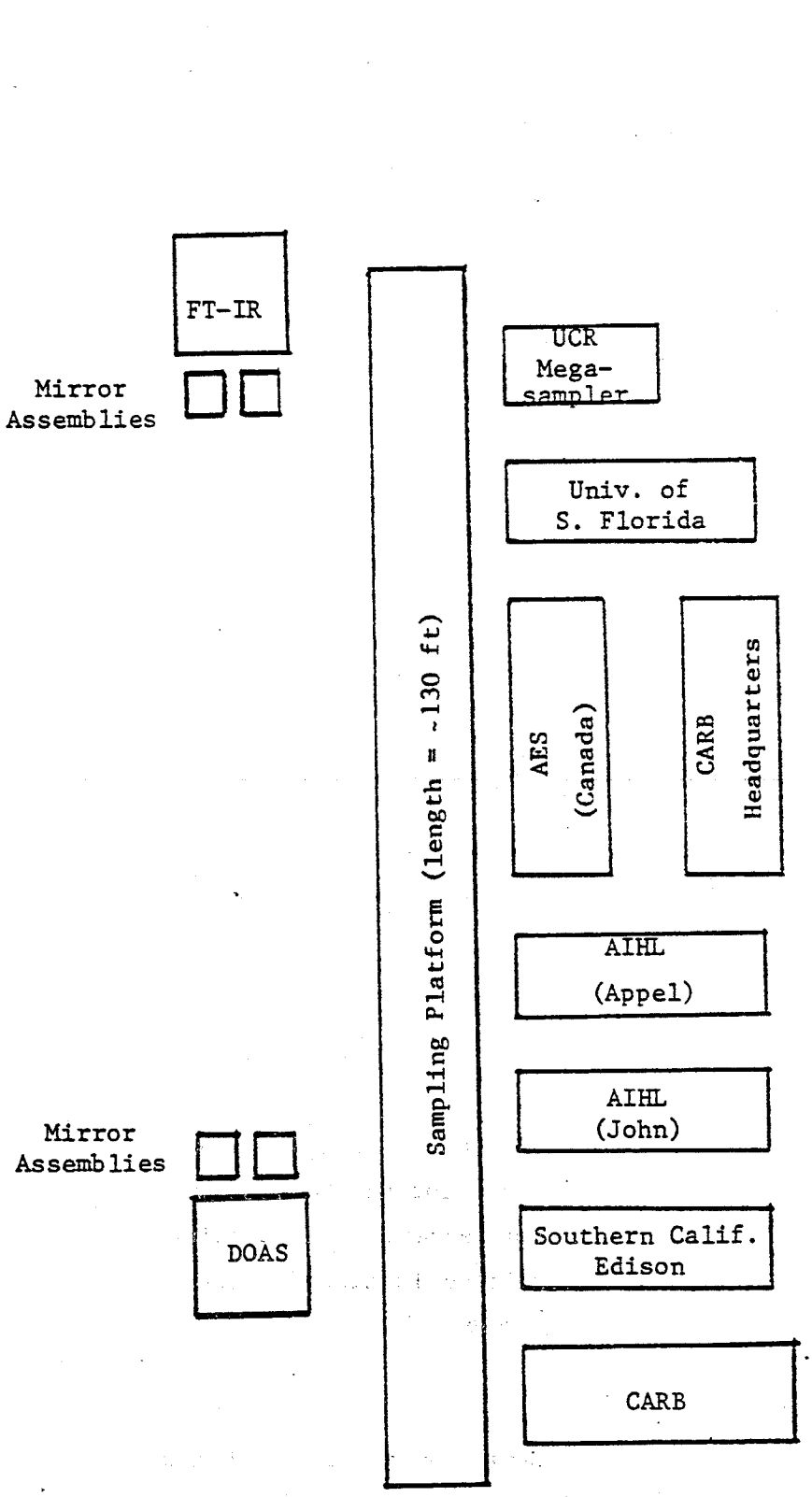

Figure III-2. Layout of the field study site illustrating the positions of the longpath FT-IR and DOAS spectrometers relative to the instruments of the other participants.

as well as separated operation of like samplers, etc. The FT-IR and DOAS measurements were unaffected by such sampling considerations since the time resolution of four to five spectra per hour for both instruments enabled them to function as "continuous" monitors for the purpose of this study.

The intercomparison study began at 0800 PDT, September 11 and lasted until 0600 PDT, September 19, 1985. For most of the analytical techniques, there were five sampling blocks for each day, namely 0000-0600, 0800-1200, 1200-1600, 1600-2000, and 2100-2400 PDT, with the period 0600-0800 being generally utilized for maintenance and calibration.

Support instrumentation for continuous monitoring of O_3, NO_x, temperature and relative humidity and wind speed and direction were operated for the duration of the study by several of the research groups at the site.

D. Operation of the Kilometer Pathlength FT-IR Spectrometer

1. Optical Alignment

Detailed attention was paid to the accuracy and stability of optical alignment as they are prerequisites to the proper operation of interferometric instruments. Design considerations such as the proper aspheric ratio (diameter vs. thickness) of the multiple-reflection mirrors, kinematic mountings and the use of massive concrete blocks as support for the interferometer and mirror system were employed to maximize optical stability.

Prior to routine operation, the accuracy of alignment was established by first installing a quartz beam splitter (which has the same geometry as the Ge/KBr beam splitter normally used for measurements). Next it was verified that the collimated beam input to the interferometer was in exact coincidence with the interferometer's optical axis, the criterion being that the return beam was focussed back onto the iris aperture and/or source element (see Figure III-1). A significant deviation of the input beam from the optical axis would result in appreciable degradation in resolution and shifts in spectral frequency.

The initial alignment of the multiple-reflection optics with respect to the interferometer was made by directing a He-Ne laser beam in reverse, from the detector position through the multi-pass optics, the quartz beam

splitter, to the iris aperature and source. Having fixed the positions of the set of mirrors between the interferometer and the multi-pass mirror system, the laser was then fixed in place such that its beam could traverse, starting from within that set of mirrors, in exact colinearity with the output beam of the interferometer all the way to the detector. This was accomplished by an additional pair of flat mirrors (these mirrors and the alignment laser are not shown in Figure III-1), one of which was within the path of the infrared beam but could be removed and repositioned reproducibly when the alignment laser was needed.

Since no visible component of light could pass through the Ge/KBr beam splitter normally used, and since even for the quartz beam splitter the light beam is too weak to be useful except in total darkness, the procedure described above constitutes the most positive check of alignment at any given time. Likewise, counting the number of dots produced by the alignment He-Ne laser on the in-focus mirror of the multiple-reflection optical system is the most positive verification of the number of beam traversals.

2. Routine Monitoring

Spectra were recorded at a pathlength of 1150 meters and 0.125 cm^{-1} resolution (unapodized). Sixty-four scans (interferograms) were co-added during a 4.5-min period and transformed to a single beam spectrum (calculation time of ~2.5 min). Each spectrum of 128 K points was truncated and only the spectral region from 400 to 1600 cm^{-1}, which contains the analytical absorption bands of HNO_3 and NH_3, was retained and archived. With the above scan conditions, four to five spectra per hour were collected.

The achievable rate of data collection permitted a cursory examination of the quality of spectra being recorded and such checks were consistently made during daytime and early evening hours (0800-2200 PDT). During the "noncritical" period of 2200-0600 hours when nitric acid was expected to be below the detection limit, the FT-IR spectrometer was programmed to conduct monitoring without operator intervention. Since this procedure essentially filled the available storage area of the computer disk, the operator was required to transfer the data onto floppy disks or magnetic tapes well ahead of the next day's start of sampling at 0800 PDT.

E. Treatment of Data and Calibration

A single beam spectrum taken at 1150 m and 0.125 cm^{-1} resolution and plotted in the 600-1500 cm^{-1} range is presented in Figure III-3. The segment of data actually stored for analysis was 400-1600 cm^{-1}, which was less than 1/6 the length of the original spectrum derived from the sampled data points. The usable transmission window at ~750-1300 cm^{-1} is still closely packed with atmospheric absorption lines, the strongest and great majority of which are due to H_2O vapor but with contributions also from CO_2 and CH_4 absorptions. A significant portion of the baseline representing zero energy (zero transmission) is included in archiving, since it is a practical test of the linearity of detector response and because a grossly distorted baseline may represent a serious failure during data sampling.

Figure III-4 illustrates the general region where the absorption features of HNO_3 and NH_3 which are most appropriate for long-path FT-IR measurements are found. A more expanded plot of the HNO_3 spectrum in the range 870-910 cm^{-1} is presented in Figure III-5, to which is added a qualitative single beam spectrum of relatively clean air at a pathlength of 1150 m. The sharp features at 896.1 and 885.4 cm^{-1} are clearly the bands of choice for analytical purposes since atmospheric interferences are minimal. Although the 878.9 cm^{-1} Q-branch is about twice as intense, it is severely overlapped by a strong water line.

Of the numerous sharp features of NH_3 absorption depicted in Figure III-4, the lines at 1103.4 and 867.9 cm^{-1}, though not among the strongest, are the least interfered by H_2O and CO_2 absorption lines and are therefore the ones chosen for analysis. The line positions of NH_3 relative to those of atmospheric H_2O (and CO_2) in the 1080-1120 cm^{-1} region are depicted in Figure III-6.

Calibration for NH_3 was straightforward. Spectra were recorded at 0.125 cm^{-1} resolution for several NH_3 pressures in the range 0.1-1 torr, as measured with an MKS Baratron capacitance manometer, in a 25-cm cell with KBr windows and pressurized with N_2 gas to atmospheric pressure. These data yielded absorption coefficients (base 10) at 23°C and 740 torr total pressure of 18.2 cm^{-1} atm^{-1} for the 1103.4 cm^{-1} peak and 9.7 cm^{-1} atm^{-1} for the 867.9 cm^{-1} peak, with less than 3% error for both values.

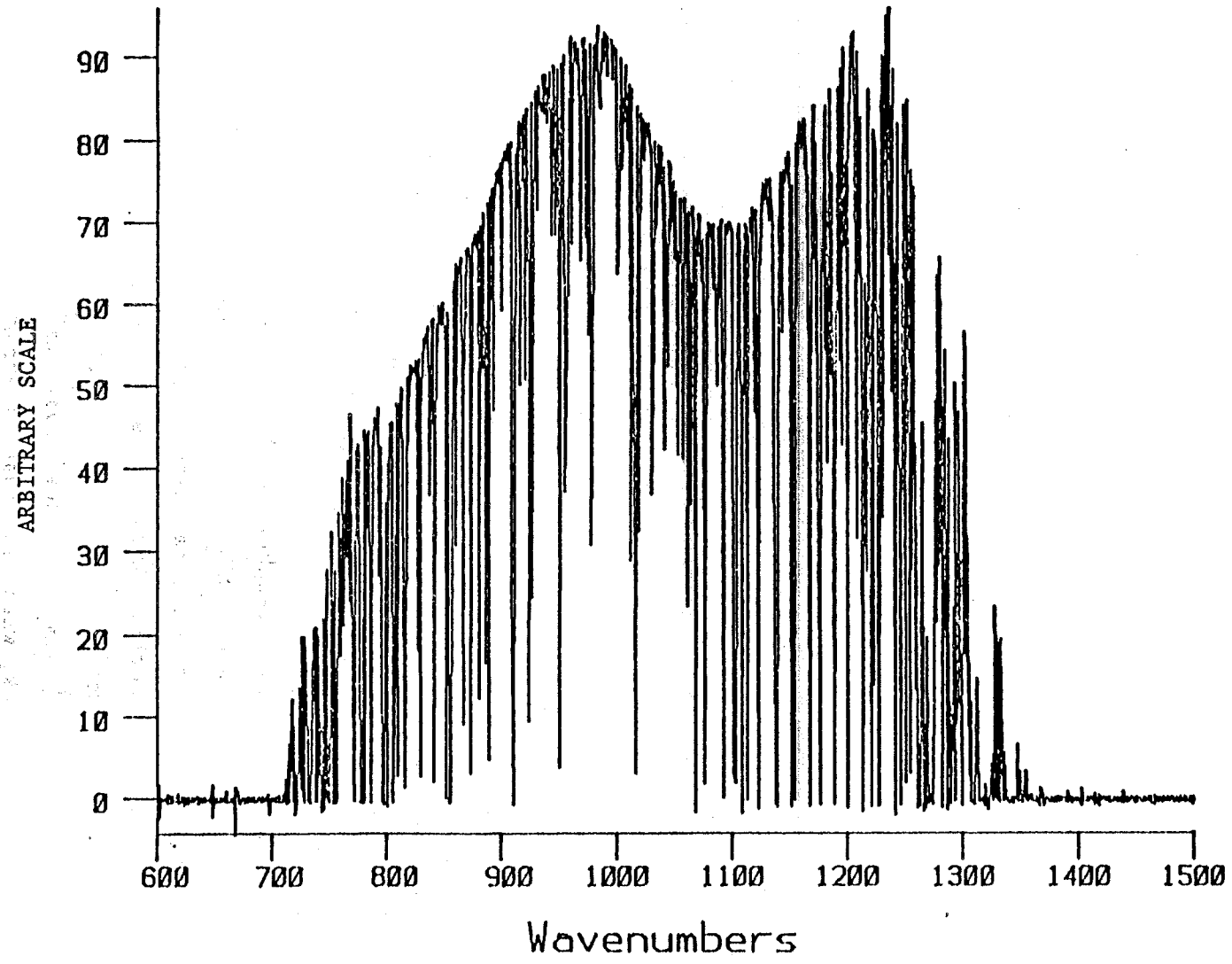

Figure III-3. Single beam spectrum of ambient air at 1150 m pathlength and 0.125 cm^{-1} resolution.

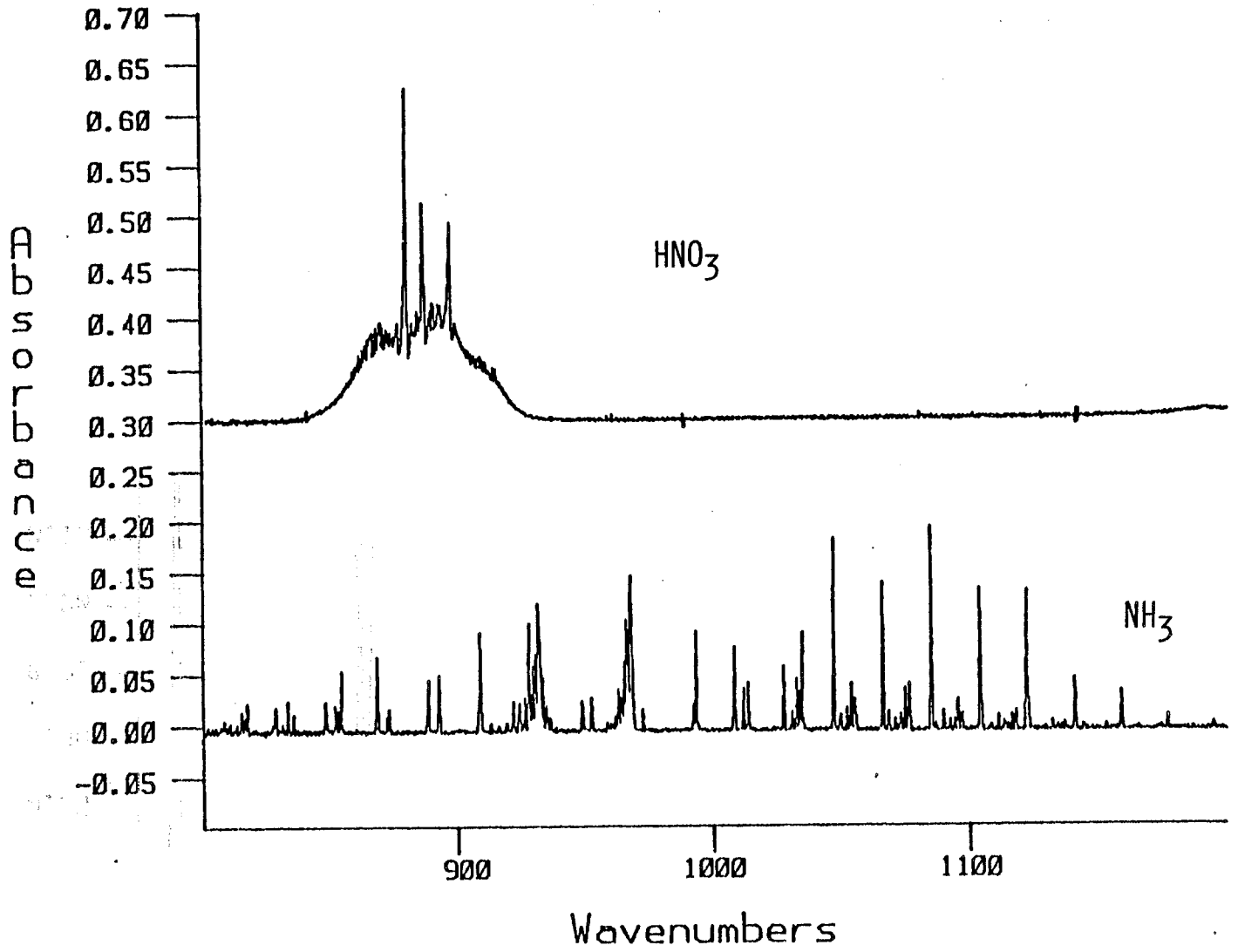

Figure III-4. Reference spectra of gaseous HNO_3 (0.61 torr) and NH_3 (0.23 torr) at spectral resolution of 0.125 cm^{-1}, pathlength of 25 cm, total pressure with N_2 of 740 torr. The HNO_3 plot is offset by 0.30 absorbance (base 10) unit for clarity.

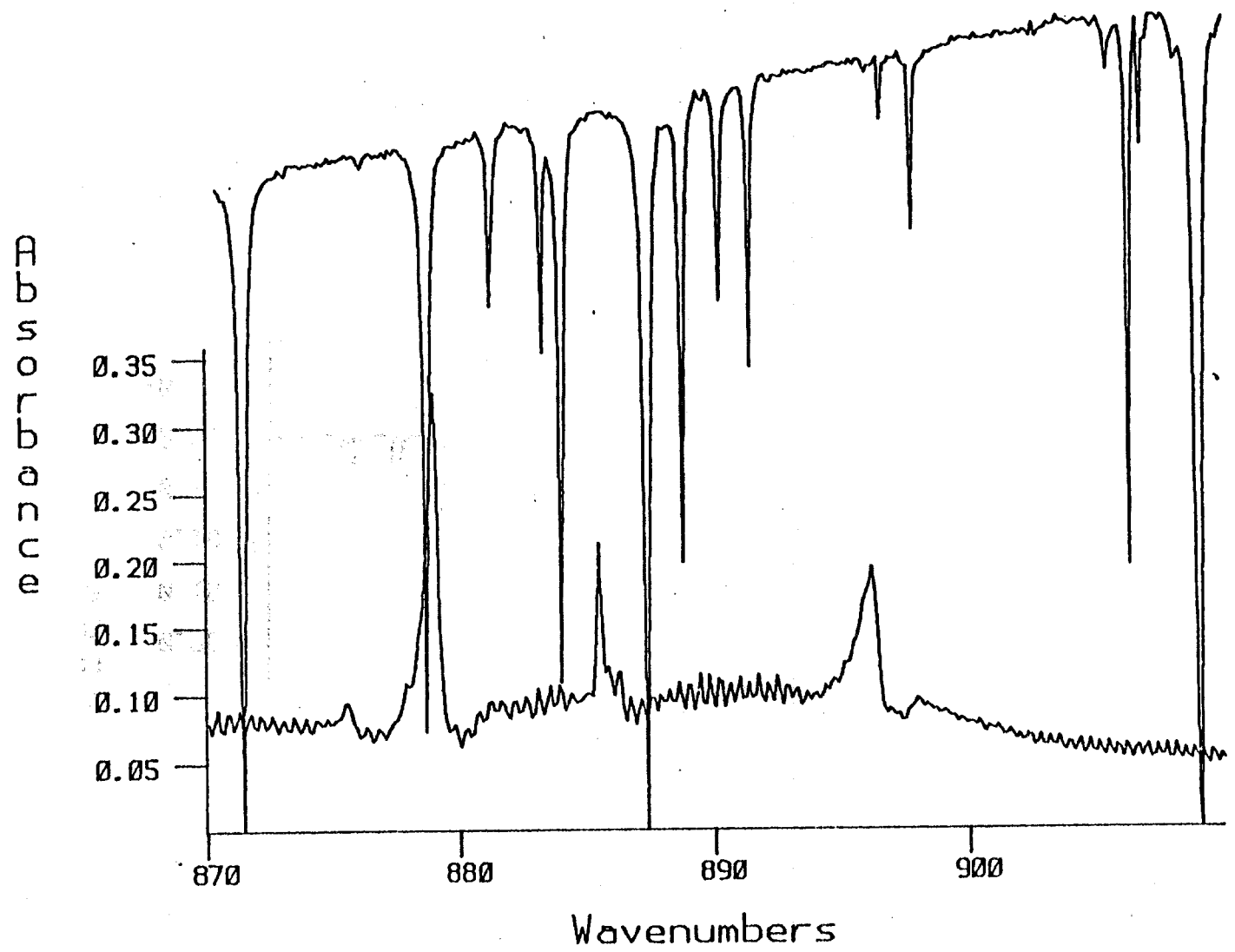

Figure III-5. Infrared absorption peaks of HNO_3 (lower trace) relative to atmospheric H_2O absorptions (upper trace) in the 870-910 cm^{-1} region.

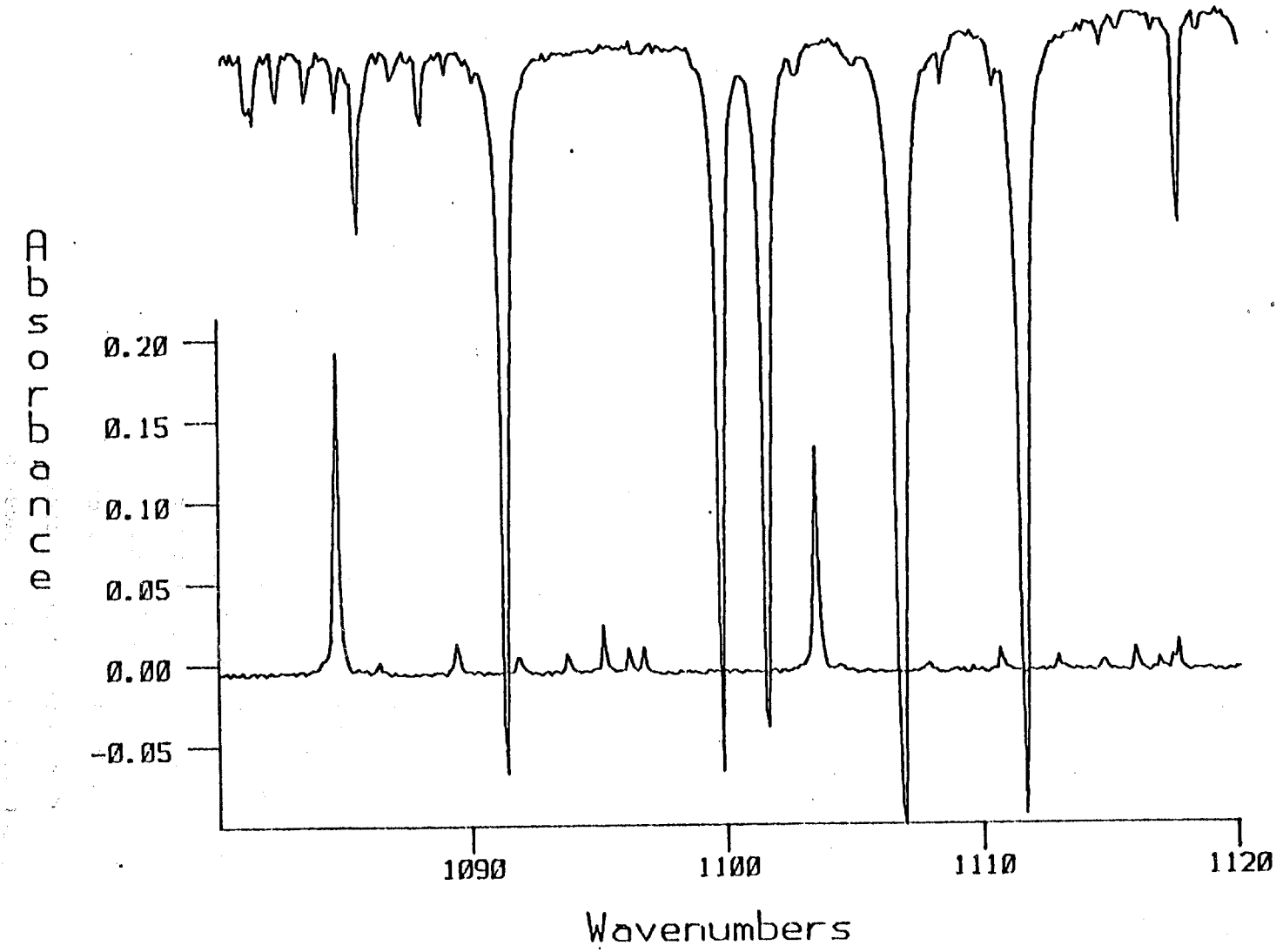

Figure III-6. Infrared absorption peaks of NH_3 (lower trace) relative to atmospheric H_2O and CO_2 absorptions (upper trace) in the 1080-1120 cm^{-1} region.

A similar calibration procedure was not possible with HNO_3 because of its significant decay to the wall of the 25-cm cell. An accurate determination of the absorption coefficient of the HNO_3 ν_4 (1325 cm^{-1}) fundamental band at ~2 cm^{-1} resolution, using two independent methods for generating HNO_3, has been reported by Graham and Johnston (1978) (see also Graham 1975). We determined our high resolution values of absorption coefficients relative to Graham and Johnston's data by comparison of broad spectral features, in particular, the ν_4 P-branch at 1315 cm^{-1}. Measurements were carried out in which 2 cm^{-1} and 0.125 cm^{-1} resolution spectra were recorded alternately for each HNO_3 sample in a 25-cm cell. The 1315 cm^{-1} peak heights at 2 cm^{-1} resolution were plotted against time as were the 0.125 cm^{-1} spectra after having been smoothed to ~2 cm^{-1} resolution. As expected, the two curves were found to be indistinguishable, permitting confident assignments of concentrations for the recorded 0.125 cm^{-1} resolution spectra. These data yielded values of 5.2 cm^{-1} atm^{-1} and 6.0 cm^{-1} atm^{-1} for the absorption coefficients (base 10) of the HNO_3 peaks at 896.1 cm^{-1} and 885.4 cm^{-1}, respectively. These values were determined for the heights of the sharp absorption ("Q branch") features only, since measurements which include the broad underlying envelope are more susceptible to unknown interferences.

The quantitative analysis of species such as HNO_3 and NH_3, which possess relatively narrow Q-branch features, sufficiently resolved from atmospheric H_2O absorptions, is normally straightforward. The absorbance ($\log I_o/I$) can be derived directly from the single beam spectrum, i.e., a ratio plot against an actual background spectrum is not necessary. Provided that the detector has a linear response, I_o and I as determined from a single beam spectrum have values on a (arbitrary) scale in which zero corresponds to no signal on the detector. The appropriate differential absorption coefficient such as those determined above must be applied to the absorption intensity measured between I_o and I. This was the procedure followed for the 1103.4 and 867.9 cm^{-1} lines of NH_3 and the 885.4 cm^{-1} peak of HNO_3. This same procedure could also be applied to the 896.1 cm^{-1} peak of HNO_3 but with more care because of slight interference from a weak H_2O line. However, the analysis of the 896.1 cm^{-1} peak was more reliably carried out by ratioing the sample spectrum with a clean background spectrum (usually the one recorded at about midnight) which

resulted in near complete cancellation of the H_2O interference and a better baseline.

Detection sensitivities were typically 3-5 ppb of HNO_3 and 1-2 ppb of NH_3. The lower detection limit for each compound was realized when turbulence due to temperature gradients and/or wind were minimal.

IV. RESULTS AND DISCUSSION

A. FT-IR Measurements

Nitric Acid. The hourly average HNO_3 concentrations (in ppb) measured by longpath FT-IR spectroscopy are summarized in Table IV-1. It can be seen that the field study period was characterized mainly by low pollution days, with HNO_3 levels mostly below the detection limit of 4 ppb. The dearth of sufficiently high levels of HNO_3 for FT-IR detection was compounded by intermittent noise problems which plagued the FT-IR measurements early in the study. Where a significant proportion of spectra in a time block are affected seriously by noise, only an upper limit average concentration of HNO_3 is given in Table IV-1. Efforts to identify the source of the interfering noise proved futile. In fact, on the evening of September 13, the problem became so severe that even the moderately strong atmospheric H_2O lines were unrecognizable, forcing a shutdown of the instrument until the next day. Fortunately, no severe noise interferences occurred on September 14 when the highest daily maximum oxidant level ($[O_3]$ >0.2 ppm) during the study was recorded. Inasmuch as HNO_3 concentrations are strongly correlated with those of O_3 (Tuazon et al. 1981, Spicer et al. 1982) the levels of HNO_3 were indeed the highest during this day, being above the FT-IR detection limit most of the daytime hours.

Figure IV-1 illustrates the detection of HNO_3 on September 14, which includes the highest value of 26 ppb recorded at 1545 hr, nearly coincident with the peak O_3 level. To facilitate comparison on the same scale, the spectra were ratioed against a common background of "clean" air, in this case a spectrum recorded at 0026 hr of September 18 when pollution levels were known to be low. Although it is nearly impossible (nor is it necessary) to ratio out completely the very strong lines of H_2O, the slight interference of a very weak H_2O line on the 896.1 cm^{-1} peak (see Figure III-5) could almost always be eliminated by this technique. The 885.4 cm^{-1} peak is much narrower than the 896.1 cm^{-1} peak, and although the former is free of interfering atmospheric absorptions and is slightly more intense, the latter is a more reliable measure of HNO_3 since its shape is much less subject to distortion by noise spikes. In any case, HNO_3 concentrations were primarily determined from ratioed spectra such

Table IV-1. Hourly Average HNO_3 Concentrations (ppb)[a,b,c] by Long Pathlength FT-IR Spectroscopy

Hourly Period (PDT)	Sept 11	Sept 12	Sept 13	Sept 14[d]	Sept 15	Sept 16	Sept 17[d]	Sept 18
0800-0900	BD	BD	BD	BD	BD	BD	BD	BD
0900-1000	BD	BD	BD	BD	BD	BD	BD	BD
1000-1100	BD	BD	BD	6.7	BD	BD	BD	BD
1100-1200	BD	BD	BD	11.2	≤4.0	BD	BD	BD
1200-1300	BD	BD	XX	13.6	≤6.3	BD	BD	BD
1300-1400	BD	BD	≤10.9	12.8	≤9.5	BD	3.3	BD
1400-1500	BD	BD	≤10.6	12.8	XX	≤4.9	7.8	BD
1500-1600	BD	XX	≤13.4	21.4	≤8.8	≤3.5	6.7	BD
1600-1700	BD	XX	≤11.8	19.2	≤6.7	BD	3.6	BD
1700-1800	BD	≤8.3	XX	8.7	XX	BD	BD	BD
1800-1900	BD	≤7.3	XX	BD	XX	BD	BD	BD
1900-2000	BD	BD	XX	BD	BD	BD	BD	BD
2000-2100	BD	BD	XX	BD	BD	BD	BD	BD
2100-2200	BD	BD	XX	BD	BD	BD	BD	BD

[a] At 23°C and 740 torr.
[b] Concentrations for periods earlier and later than the time periods shown are below detection limit (<4 ppb).
[c] BD: Below detection; XX indicates indeterminate concentration due to very high noise level in the spectra; ≤ symbol designates an upper limit estimate (dictated by the presence of significant noise in some of the spectra in the data set). Digits beyond 2 significant figures are retained only for the sake of format.
[d] Error: ±4 ppb.

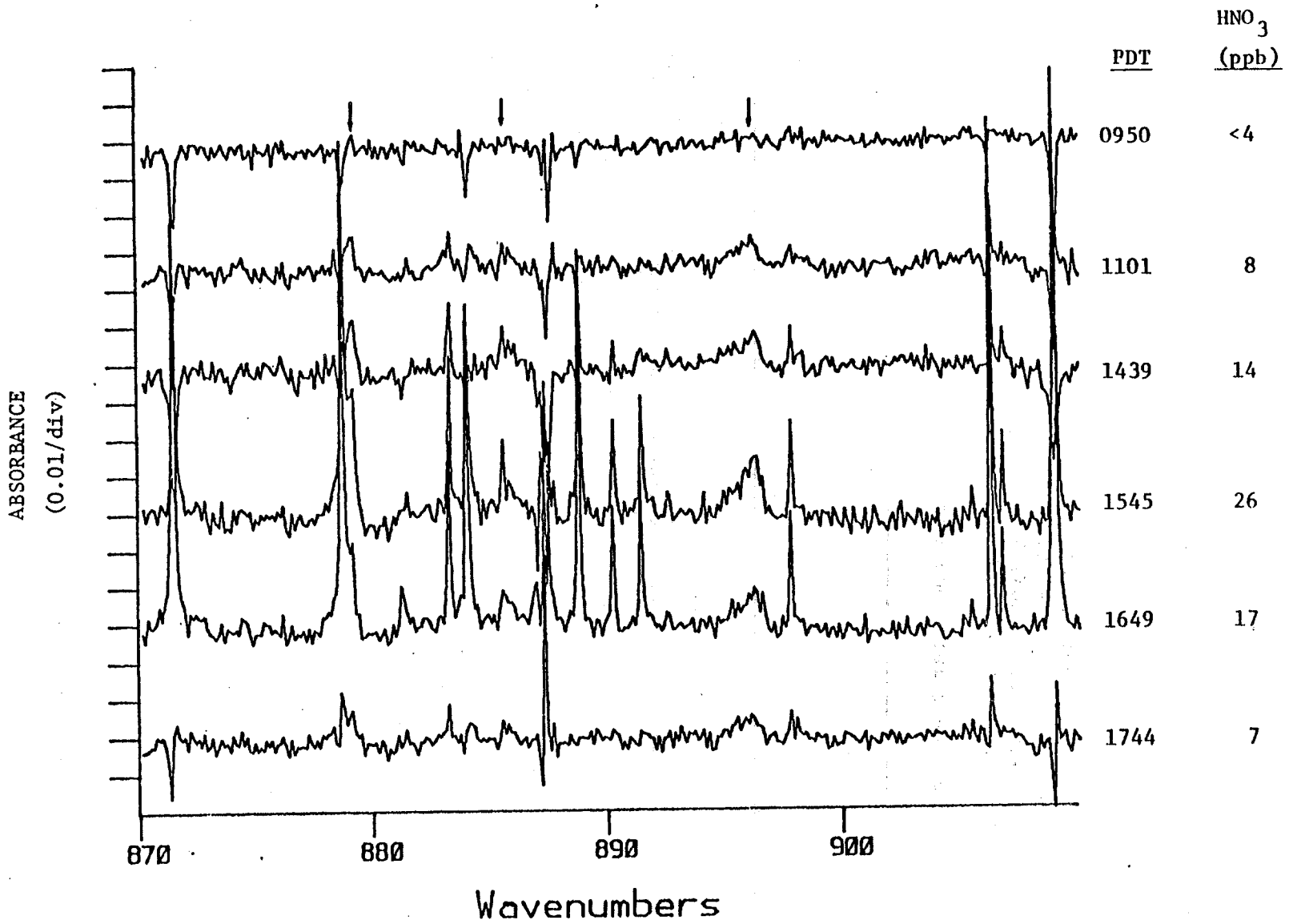

Figure IV-1. FT-IR spectroscopic detection of HNO_3 during the pollution episode of September 14, 1985 in Claremont, CA. The arrows indicate the positions of the HNO_3 absorption peaks.

as those illustrated in Figure IV-1, with the 896.1 cm^{-1} peak as the main criterion and with additional verification from the 885.4 cm^{-1} absorption when possible.

It should be noted that the absorption coefficient of 5.2 cm^{-1} atm^{-1} for the 896.1 cm^{-1} peak is the same for the present spectral resolution of 0.125 cm^{-1} as it is for 0.5 cm^{-1} resolution, the latter being the resolution employed in our previous studies (Tuazon et al. 1978, 1980, 1981). Indeed, smoothing the spectra shown in Figure IV-1 down to an approximate 0.5 cm^{-1} resolution caused no change in the intensity of the 896.1 cm^{-1} peak but brought about a measurable reduction in the apparent noise. For this reason the errors encountered here in the measurement of the 896.1 cm^{-1} peak at 0.125 cm^{-1} spectral resolution must be considered upper limit errors.

The measurement errors are generally within ±4 ppb for the spectra which are not affected by the unusual interference problem mentioned earlier. For a number of hourly periods, designated XX in Table IV-1, severe noise levels in the spectra yielded errors greater than two or three times the above error limit, thus making the measurements indeterminate. In several cases, measurements during a one-hour period consisted of "normal" scans as well as moderately noisy spectra. Concentrations for these periods are reported as upper limit values because of the inherent tendency to overestimate absorption intensities in the presence of noise.

The best FT-IR data for comparison with other continuous methods (e.g., diode laser spectroscopy) are those obtained during September 14 and September 17. In addition to the hourly average HNO_3 concentrations for these two days, which are included in Table IV-1, the detailed time-concentration data for September 14 and September 17 are presented in Table IV-2 and Table IV-3, respectively. As noted earlier, HNO_3 levels down to 3 ppb could be measured in favorable cases. This explains the occurrence in Table IV-1, as well as in Table IV-3, of average concentrations which are less than the nominal detection limit of 4 ppb.

To facilitate comparison with other measurement methods (filter packs, denuder difference, annular denuder, etc.) the average concentration for the designated sampling blocks were derived from the hourly averages (where data are sufficient) and presented in Table IV-4. Values

Table IV-2. HNO_3 Concentration (ppb)[a,b,c] vs. Time in Claremont, CA, on September 14, 1985 by Long Pathlength FT-IR Spectroscopy

PDT	HNO_3 (ppb)	PDT	HNO_3 (ppb)
0927	<4	1354	10.9
0937	<4	1410	11.7
0950	<4	1423	11.7
1009	6.3	1439	13.9
1023	7.0	1452	13.4
1035	6.7	1507	18.4
1049	7.5	1520	20.0
1101	8.4	1531	21.7
1112	8.7	1545	25.9
1124	12.0	1559	21.4
1141	10.9	1615	20.0
1154	14.2	1629	20.0
1208	14.0	1649	16.7
1224	15.0	1703	15.5
1239	13.7	1717	8.4
1251	11.7	1729	8.4
1304	11.4	1744	6.7
1316	13.4	1816	<4
1329	15.9	1827	<4
1342	11.7	1840	<4

[a]At 23°C and 740 torr.
[b]Digits beyond two significant figures are retained only for the sake of format.
[c]Error: ±4 ppb.

Table IV-3. HNO_3 Concentration (ppb)[a,b] vs. Time in Claremont, CA, on September 17, 1985 by Long Pathlength FT-IR Spectroscopy

PDT	HNO_3 (ppb)	PDT	HNO_3 (ppb)
1208	<3	1518	8.7
1219	<3	1532	5.8
1231	<3	1542	3.4
1245	<3	1554	7.5
1257	4.6	1606	3.3
1309	<3	1619	3.3
1331	4.3	1632	6.0
1343	5.0	1653	3.7
1356	6.2	1706	4.2
1418	8.0	1723	<3
1431	6.7	1735	<3
1442	9.2	1753	<3
1453	8.4	1803	<4
1505	8.3		

[a]At 23°C and 740 torr.
[b]Error: ±4 ppb.

Table IV-4. Average HNO_3 Concentrations (ppb)[a,b,c] by Long Pathlength FT-IR Spectroscopy for the Designated Sampling Periods

Sampling Period (PDT)	Sept 11	Sept 12	Sept 13	Sept 14	Sept 15	Sept 16	Sept 17	Sept 18	Sept 19
0000-0600		-	<4	-	<4	<4	<4	<4	<4
0800-1200	<4	<4	<4	4.5-6.5	<4	<4	<4	<4	
1200-1600	<4	<4	(10.1)	15.2	(8.4)	(2.1-4.1)	4.5-5.5	<4	
1600-2000	<4	XX	XX	7.0-9.0	XX	<4	<4	<4	
2000-2400	<4	<4	-	<4	<4	<4	<4	<4	

[a]Dash means incomplete or no data; XX designates an indeterminate value due to the presence of excessive noise levels in a significant number of spectra in the block.
[b]See text for the method used in estimating the concentration range for a particular block.
[c]An error of ±4 ppb applies to the values or range of values for September 14 and 17; this error does not apply to the values in parentheses which were largely derived from upper limit hourly concentrations (Table IV-1).

below detection limit are represented as <4 ppb. When the number of hourly averages above detection limit is at least equal to the number of values below detection (BD) within a block, a lower limit and an upper limit average are calculated by substituting 0 and 4, respectively, for BD in Table IV-1. This is easily done for the relevant data of September 14 and 17. The values for the 1200-1600 hr blocks of September 13, 15 and 16 are similarly calculated with some interpolation of data, but must be regarded as less reliable due to the larger uncertainties of the hourly averages from which they were derived.

Ammonia. The measurement of NH_3 is important because this compound reacts with gaseous HNO_3 to form particulate NH_4NO_3. The occurrence of NH_3 at significant levels in the eastern part of the CSCAB has been postulated as the reason for low observed HNO_3 levels, even during moderate to

severe smog episodes, and corresponding high particulate nitrate levels (Doyle et al. 1979, Tuazon et al. 1980). The analysis of NH_3 by FT-IR spectroscopy was more conveniently carried out than for HNO_3, since the NH_3 measurement peaks at 1103.4 and 867.9 cm^{-1} are more intense and free of common atmospheric interferences. Hence, NH_3 measurements were directly obtained from the single beam spectra.

The ammonia data obtained during the eight-day period are given in Table IV-5. They indicate that 2-4 ppb was a common background level of NH_3 in Claremont during the field study period. Particularly high concentrations of NH_3 were observed in the morning hours of September 16 and 17 and early afternoon of September 12 when maximum hourly average concentrations of 33, 46 and 57 ppb, respectively, were measured. These coincided with prevailing winds from the south or southeast, which can transport high levels of NH_3 to Claremont from the predominantly agricultural areas, containing poultry and dairy farms and feed lots, of Chino and Ontario (~7-9 miles away). The average NH_3 concentrations for the five designated sampling blocks are presented in Table IV-6.

Figure IV-2 presents single-beam spectra recorded on the morning of September 16 in which the NH_3 concentration rapidly changed from below the detection limit (<1.5 ppb) at 8:19 a.m., to 18 ppb at 8:31 a.m., and to 84 ppb at 8:56 a.m., the latter instantaneous value being the highest NH_3 concentration recorded by the longpath FT-IR technique during this study.

The HNO_3 concentrations given in Table IV-1, and a portion of the NH_3 data in Table IV-3, were submitted in preliminary form to Drs. Douglas Lawson (ARB) and Susanne Hering (UCLA), the intercomparison study project coordinators. Upon their request these data were expressed in the concentration unit nanomoles per cubic meter (1 ppb = 40 nanomoles m^{-3} at 23°C and 740 torr). Values of the FT-IR data expressed in this unit are provided in Appendices A and B, as are the average HNO_3 and NH_3 concentrations for the designated time blocks (Appendices C and D).

Table IV-5. Hourly Average NH_3 Concentrations (ppb)[a,b,c] by Long Pathlength FT-IR Spectroscopy

Hourly Period (PDT)	Sept 11	Sept 12	Sept 13	Sept 14	Sept 15	Sept 16	Sept 17	Sept 18	Sept 19
0000-0100		-	3.5	-	2.2	2.3	1.5	1.9	1.9
0100-0200		-	3.4	-	3.5	2.3	1.7	2.2	1.8
0200-0300		-	3.2	-	2.5	2.9	1.9	2.2	1.5
0300-0400		-	3.0	-	2.8	2.2	1.2	3.3	1.4
0400-0500		-	2.9	-	2.6	1.7	5.3	2.8	1.8
0500-0600		-	2.4	-	2.1	1.2	10.8	4.0	2.1
0800-0900	1.9	3.8	6.0	4.2	5.6	31.6	15.2	2.8	
0900-1000	2.8	5.4	6.6	4.4	5.7	23.4	17.3	2.0	
1000-1100	2.8	6.2	10.5	3.9	6.3	22.5	46.2	2.4	
1100-1200	2.2	4.9	33.6	3.6	6.9	33.3	39.7	2.0	
1200-1300	1.5	15.3	16.1[d]	4.7	7.3	17.8	21.0	1.9	
1300-1400	1.7	42.4	7.6	4.0	6.5	6.0	6.0	1.0	
1400-1500	2.5	57.0	4.6	4.7	5.2[d]	4.6	3.6	2.5	
1500-1600	2.4	14.5[d]	4.6	3.8	4.3	3.2	2.9	3.0	
1600-1700	1.8	8.1[d]	4.0	4.0	4.2	4.0	3.6	3.1	
1700-1800	2.3	4.9	4.3[d]	4.9	3.4[d]	3.0	2.7	4.1	
1800-1900	2.8	4.8	XX	4.6	3.5[d]	3.4	2.1	4.3	
1900-2000	3.2	6.0	XX	5.6	4.1	3.1	2.3	2.9	
2000-2100	3.9	5.3	XX	4.3	4.8	3.3	3.4	3.5	
2100-2200	2.8	6.5	XX	4.8	2.3	3.0	3.3	2.5	
2200-2300	-	4.0	-	3.4	3.4	-	3.4	2.6	
2300-2400	-	3.6	-	3.0	3.1	-	2.6	2.6	

[a]At 23°C and 740 torr.
[b]Error: ±1.5 ppb; detection sensitivity = 1.5 ppb. Digits beyond 2 significant figures are retained only for the sake of format.
[c]Dash designates no data; XX indicates indeterminate concentrations due to very high noise levels in the spectra.
[d]A higher error limit of ±2.5 ppb has been estimated for these periods.

Table IV-6. Average NH_3 Concentrations (ppb)[a] by Long Pathlength FT-IR Spectroscopy for the Designated Sampling Periods

Sampling Period (PDT)	Sept 11	Sept 12	Sept 13	Sept 14	Sept 15	Sept 16	Sept 17	Sept 18	Sept 19
0000-0600		-	3.1	-	2.6	2.1	3.7	2.7	1.7
0800-1200	2.4	5.1	14.2	4.0	6.1	27.7	29.6	2.3	
1200-1600	2.0	32.3[b]	8.2[b]	4.3	5.8[b]	7.9	8.4	2.1	
1600-2000	2.5	6.0[b]	XX	4.8	3.8[b]	3.4	2.7	3.6	
2000-2400	-	4.8	-	3.9	3.4	-	3.2	2.8	

[a]Dash means incomplete or no data; XX designates an indeterminate concentration due to the presence of excessive noise in a significant number of spectra in the block. Error = ±1.5 ppb unless noted otherwise.
[b]An uncertainty of ±2 ppb applies to these values.

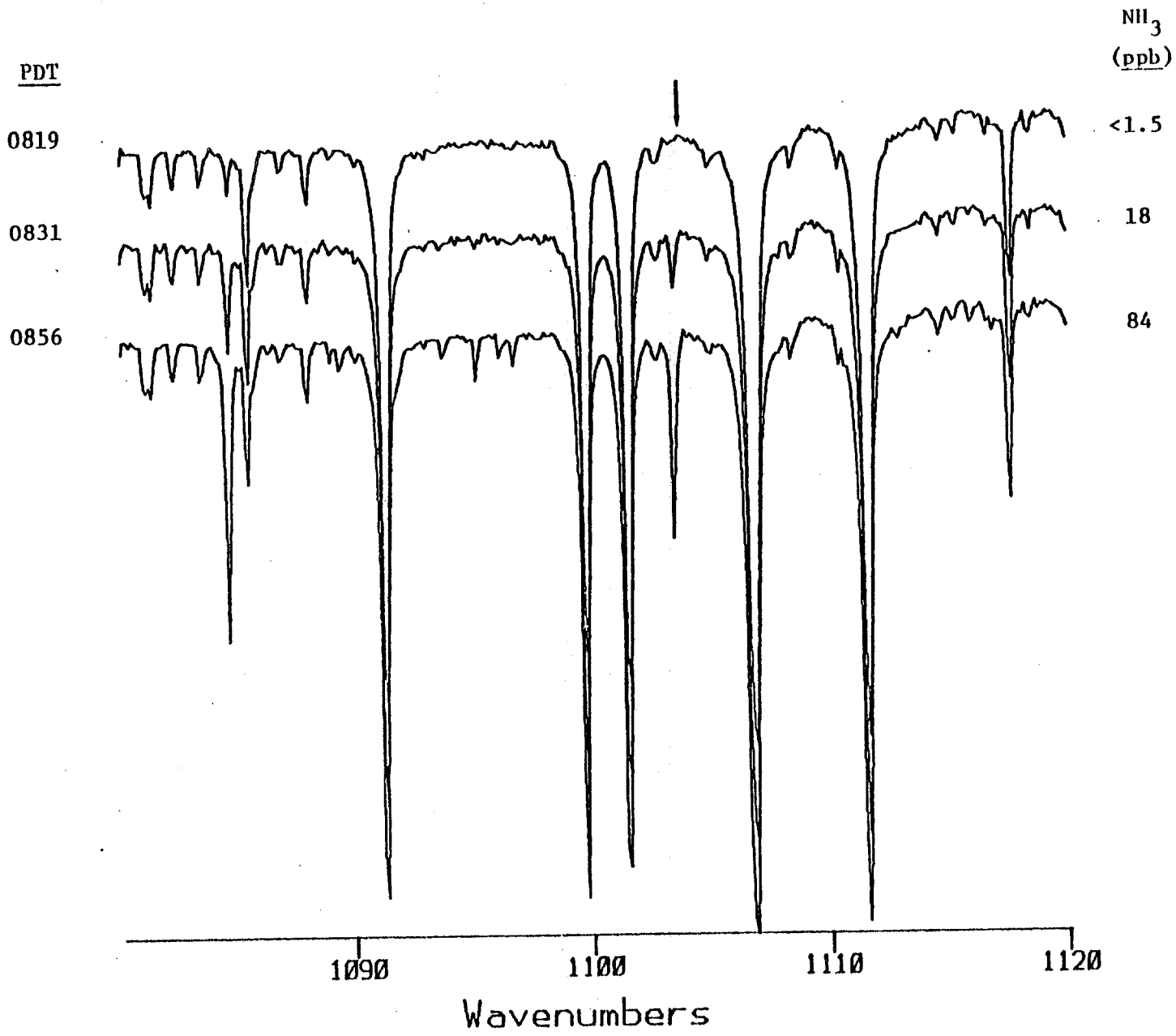

Figure IV-2. FT-IR spectroscopic detection of NH_3 in Claremont, CA, on September 16, 1985. The arrow indicates the measurement peak of NH_3 at 1103.4 cm^{-1}.

B. DOAS Measurements

Supplementary data for NO_2 and HONO concentrations as measured by our long pathlength DOAS system are provided in Tables IV-7 and IV-8. As discussed earlier, these data are properly assigned to another SAPRC-ARB program (Contract No. A4-081-32) and will be reported in detail in the final report to that project.

The practical detection limit of the DOAS system corresponded to an optical density of about 1.5×10^{-4} (base 10), which at the 800 m pathlength employed gave sensitivities of 4 ppb NO_2, 0.6 ppb HONO and 0.02 ppb NO_3. NO_3 radical concentrations never exceeded the detection limit except on September 13 and 14 for a one-hour period on each day around 8 p.m. when the concentration peaked at about 70 parts per trillion (ppt).

Error limits for the NO_2 data have been estimated at ±15% or ±2 ppb, whichever is larger. Taking into account that NO_2 had to be subtracted from the DOAS spectrum prior to a HONO measurement, the error limits for the HONO data have been estimated as ±30% or ±0.6 ppb, whichever is higher, plus ±0.5% of the NO_2 concentration present at that time. Such compounded error limits correspond to a worst case calculation; the subtraction of the NO_2 bands can usually be performed with much higher precision.

The data in Tables IV-7 and IV-8 are hourly averages computed from the original measurements which cover 12-minute sampling intervals. When concentration levels were detectable only for part of the hour they were quoted as upper limits. For example, based on a detection limit of 0.6 ppb, if during the first 48 minutes (four 12-minute samples) no HONO was detected and for the last 12 minutes a concentration of 0.65 ppb was measured, an upper limit of $[(4 \times 0.6) + 0.65]/5 = 0.61$ ppb would be quoted. A precision of two decimal places has been maintained throughout the listing for HONO to reduce roundoff errors in further calculations.

NO_2 levels were always above the detection limit of 4 ppb with a minimum value of 9 ppb observed during the early afternoon hours of September 15, and a maximum of 135 ppb recorded during the evening of September 12. Significant levels of HONO were observed during the nights of September 12/13, 13/14, 14/15 and 15/16. The highest HONO concentration of ~2.6 ppb was observed at around midnight on September 15/16.

Table IV-7. Hourly Average NO_2 Concentrations (ppb)[a] by Long Pathlength DOAS Spectroscopy

Hourly Period (PDT)	Sept 11	Sept 12	Sept 13	Sept 14	Sept 15	Sept 16	Sept 17	Sept 18	Sept 19
0000-0100		46	83	82	85	56	50	41	22
0100-0200		48	38	54	39	32	47	38	20
0200-0300		40	31	55	52	21	28	42	18
0300-0400		36	23	48	37	38	16	43	16
0400-0500		40	21	42	45	40	18	39	24
0500-0600		42	25	44	29	41	15	39	33
0600-0700		47	52	41	18	36	21	41	33
0700-0800		50	73	40	42	27	22	38	34
0800-0900	23	47	72	75	41	49	21	37	36
0900-1000	21	50	59	97	60	61	28	34	
1000-1100	20	46	53	62	40	47	33	36	
1100-1200	17	46	40	36	23	29	28	26	
1200-1300	15	26	15	39	11	21	24	25	
1300-1400	13	13	32	23	11	18	24	41	
1400-1500	15	12	26	17	9	16	20	24	
1500-1600	15	34	28	19	11	17	22	33	
1600-1700	18	33	37	27	13	21	32	39	
1700-1800	22	38	48	26	16	30	35	36	
1800-1900	29	50	58	37	34	33	46	33	
1900-2000	43	78	73	50	47	36	48	47	
2000-2100	52	123	99	58	56	40	64	45	
2100-2200	53	135	128	80	69	56	62	43	
2200-2300	52	103	119	90	73	64	57	37	
2300-2400	45	96	110	91	63	59	51	30	

[a]Estimated errors: ±4 ppb or ±15%, whichever is larger.

Table IV-8. Hourly Average HONO Concentrations (ppb)[a,b] by Long Pathlength DOAS Spectroscopy

Hourly Period (PDT)	Sept 11	Sept 12	Sept 13	Sept 14	Sept 15	Sept 16	Sept 17	Sept 18
0000-0100		0.74	1.56	1.25	1.31	2.55	0.83	BD
0100-0200		0.75	0.97	0.94	0.69	1.89	0.68	BD
0200-0300		0.73	0.74	0.88	0.89	1.37	≤0.63	≤0.66
0300-0400		0.85	0.61	0.94	0.87	1.40	BD	≤0.80
0400-0500		0.75	0.63	0.98	0.94	1.31	BD	BD
0500-0600		1.00	≤0.62	1.03	0.78	1.37	BD	BD
0600-0700		1.04	BD	0.85	0.66	1.27	BD	BD
0700-0800		≤0.82	BD	≤0.70	≤0.66	≤0.79	BD	BD
0800-0900	BD	BD	BD	BD	BD	BD	BD	BD
0900-1000	BD	BD	BD	BD	BD	BD	BD	BD
1000-1100	BD	BD	BD	BD	BD	BD	BD	BD
1100-1200	BD	BD	BD	BD	BD	BD	BD	BD
1200-1300	BD	BD	BD	BD	BD	BD	BD	BD
1300-1400	BD	BD	BD	BD	BD	BD	BD	BD
1400-1500	BD	BD	BD	BD	BD	BD	BD	BD
1500-1600	BD	BD	BD	BD	BD	BD	BD	BD
1600-1700	BD	BD	BD	BD	BD	BD	BD	BD
1700-1800	BD	BD	BD	BD	BD	BD	BD	BD
1800-1900	BD	BD	BD	BD	BD	BD	BD	BD
1900-2000	BD	BD	BD	BD	BD	BD	BD	≤0.62
2000-2100	BD	≤0.63	BD	BD	BD	BD	BD	≤0.80
2100-2200	BD	0.88	≤0.79	≤0.79	≤0.61	BD	BD	≤0.91
2200-2300	≤0.62	1.53	1.16	1.28	0.95	≤0.66	BD	≤0.64
2300-2400	0.75	1.76	1.43	1.48	1.76	1.01	BD	BD

[a] BD: below detection.
[b] Digits beyond 2 significant figures are retained only for the sake of format. See text for a discussion of errors.

Tables IV-9 and IV-10 contain the computed NO_2 and HONO concentrations averaged over the sampling periods designated for non-spectroscopic methods. These numbers were derived from the hourly averages in Tables IV-7 and IV-8.

Conclusion. The foregoing FT-IR and DOAS data are presented here as carefully evaluated compilations of data, but without the benefit of extended interpretation. Such interpretation will be conducted by the CARB staff, and by ourselves once we have access to the totality of data which were obtained in the intercomparison study. These interpretations will be presented in appropriate peer-reviewed journal articles as well as at scientific meetings (e.g., the National American Chemical Society meeting at Anaheim, CA, September 8-12).

Table IV-9. Average NO_2 Concentrations (ppb) by Long Pathlength DOAS Spectroscopy for the Designated Sampling Periods

Sampling Period (PDT)	Sept 11	Sept 12	Sept 13	Sept 14	Sept 15	Sept 16	Sept 17	Sept 18	Sept 19
0000-0600		42	37	54	48	38	29	40	22
0800-1200	20	47	56	68	41	47	28	33	
1200-1600	15	21	25	25	11	18	23	31	
1600-2000	28	50	54	35	28	30	40	39	
2000-2400	51	114	114	80	65	55	59	39	

Table IV-10. Average HONO Concentrations (ppb) by Long Pathlength DOAS Spectroscopy for the Designated Sampling Periods

Sampling Period (PDT)	Sept 11	Sept 12	Sept 13	Sept 14	Sept 15	Sept 16	Sept 17	Sept 18	Sept 19
0000-0600		0.8	0.9	1.0	0.9	1.6	$\leq$0.7	$\leq$0.6	BD
0800-1200	BD	BD	BD	BD	BD	BD	BD	BD	
1200-1600	BD	BD	BD	BD	BD	BD	BD	BD	
1600-2000	BD	BD	BD	BD	BD	BD	BD	BD	
2000-2400	$\leq$0.6	$\leq$1.2	$\leq$1.0	$\leq$1.0	$\leq$1.0	$\leq$0.7	BD	$\leq$0.9	

V. REFERENCES

Anlauf, K. G., Fellin P. and Wiebe, H. A. (1984): Characterization of several integrative sampling methods for atmospheric particles, nitric acid and sulfur dioxide. Report ARQA 117-84, Atmospheric Environment Service. Downsview, Ontario.

Anlauf, K. G., Fellin, P., Wiebe, H. A., Schiff, H. I., McKay, G. I., Braman, R. S. and R. Gilbert (1985): A comparison of three methods for measurement of atmospheric nitric acid and aerosol nitrate and ammonium. Atmos. Environ. 19, 325-333.

Appel, B. R., Tokiwa Y. and Haik, M. (1981): Sampling of nitrates in ambient air. Atmos. Environ. 15, 283-289.

Braman, R. S., Shelley, T. J. and McClenny, W. A. (1982): Tungstic acid for preconcentration and determination of gaseous and particulate ammonia and nitric acid in ambient air. Anal. Chem. 54, 358-364.

Doyle, G. D., Tuazon, E. C., Graham, R. A., Mischke, T. M., Winer, A. M. and Pitts, J. N., Jr. (1979): Simultaneous concentrations of ammonia and nitric acid in a polluted atmosphere and their equilibrium relationship to particulate ammonium nitrate. Environ. Sci. Technol. 13, 1416-1419.

Fellin, P., Wiebe, H. A. and Anlauf, K. G. (1980): Design and characterization of a low volume sampling system for the simultaneous sampling of atmospheric particles and vapor phase nitric acid. Internal Report: ARQA 83-80, Atmospheric Environment Service, Downsview, Ontario.

Forrest, J., Spandau, D. J., Tanner, R. L. and Newman, L. (1982): Determination of atmospheric nitrate and nitric acid employing a diffusion denuder with a filter pack. Atmos. Environ. 16, 1473-1485.

Gailey, P. C., McClenny, W. A., Braman, R. S. and Shelley, T. J. (1983): A simple design for automation of the tungsten (VI) oxide technique for measurement of NH_2 and HNO_3. Atmos. Environ. 17, 1517-1519.

Golden, P. D., Kuster, W. C., Albritton, D. L., Fehsenfeld, F. C., Connell, P. S., Norton, R. B. and Huebert, B. J. (1983): Calibration and tests of the filter-collection method for measuring clean-air, ambient levels of nitric acid. Atmos. Environ. 17, 1355-1364.

Graham, R. A. (1975): The photochemistry of NO_3 and the kinetics of the N_2O_5-O_3 system. Ph.D. Thesis, U.C.-Berkeley, 176 pp.

Graham, R. A. and Johnston, H. S. (1978): The photochemistry of NO_3 and the kinetics of the N_2O_5-O_3 system. J. Phys. Chem. 82, 254-268.

Hanst, P. L. (1971): Spectroscopic methods for air pollution measurements. Adv. Environ. Sci. Technol. 2, 91.

Hanst, P. L., Wong, N. W. and Bragin, J. (1984): A long-path infra-red study of Los Angeles smog. Atmos. Environ. 16, 969-981.

Horn, D. and Pimentel, G. C. (1971): 2.5 km Low-temperature multiple-reflection cell. Applied Optics 10, 1892-1898.

McClenny, W. A., Galley, P. C., Braman, R. S. and Shelley, T. J. (1982): Tungstic acid technique for monitoring nitric acid and ammonia in ambient air. Anal. Chem. 54, 365-369.

Pitts, J. N., Jr., Biermann, H. W., Atkinson, R. and Winer, A. M. (1984): Atmospheric implications of simultaneous nighttime measurements of NO_3 radicals and HONO. Geophys. Res. Lett. 11, 557-560.

Platt, U., Perner, D., Harris, G. W., Winer, A. M. and Pitts, J. N., Jr. (1980): Observations of nitrous acid in an urban atmosphere by differential optical absorption. Nature, 312-314.

Platt, U. and Perner, D. (1983): Measurement of atmospheric trace gases by longpath differential UV/visible absorption spectroscopy. In: Optical and Laser Remote Sensing, Springer-Verlag, 39, 97-105.

Schiff, H. I., Hastie, D. R., Mackay, G. I., Iguchi, T. and Ridley, B. A. (1983): Tunable diode laser systems for measuring trace gases in tropospheric air. Environ. Sci. Technol. 17, 352A-364A.

Shaw, R. W., Jr., Stevens, R. K., Bowermaster, J., Tesch, J. W. and Tew, E. (1982): Measurements of atmospheric nitrate and nitric acid: the denuder difference experiment. Atmos. Environ. 16, 845-848.

Spicer, C. W., Howes, J. E., Jr., Bishop, T. A., Arnold, L. H. and Stevens, R. K. (1982): Nitric acid measurement methods: an intercomparison. Atmos. Environ. 16, 1487-1500.

Stelson, A. W. and Seinfeld, J. H. (1982): Relative humidity and temperature dependence of the ammonium nitrate dissociation constant. Atmos. Environ. 16, 983-992.

Stevens, R. K. (Ed.) (1979): Current methods to measure atmospheric nitric acid and nitrate artifacts. U. S. Environmental Protection Agency Report No. EPA-6002-79-051, Research Triangle Park, N.C.

Tuazon, E. C., Graham, R. A., Winer, A. M., Easton, R. R., Pitts, J. N., Jr., and Hanst P. L. (1978): A kilometer pathlength Fourier-transform infrared system for the study of trace pollutants in ambient and synthetic atmospheres. Atmos. Environ. 12, 865-875.

Tuazon, E. C., Winer, A. M., Graham, R. A. and Pitts, J. N., Jr. (1980): Atmospheric measurements of trace pollutants by kilometer pathlength FT-IR spectroscopy. Adv. Environ. Sci. Technol. 10, 259-300.

Tuazon, E. C., Winer, A. M. and Pitts, J. N., Jr. (1981): Trace pollutant concentrations in a multi-day smog episode in the California South Coast Air Basin by long pathlength FT-IR spectroscopy. Environ. Sci. Technol., 15, 1232-1237.

White, J. U. (1942): Long optical paths of large aperture. J. Opt. Soc. Amer. 32, 285-288.

VI. APPENDICES

Appendix A: Hourly Average HNO_3 Concentrations (nanomoles m^{-3}) by Long Pathlength FT-IR Spectroscopy

Appendix B: Hourly Average NH_3 Concentrations (nanomoles m^{-3}) by Long Pathlength FT-IR Spectroscopy

Appendix C: Average HNO_3 Concentrations (nanomoles m^{-3}) by Long Pathlength FT-IR Spectroscopy for the Designated Sampling Periods

Appendix D: Average NH_3 Concentrations (nanomoles m^{-3}) by Long Pathlength FT-IR Spectroscopy for the Designated Sampling Periods

Appendix A

Hourly Average HNO_3 Concentrations (nanomoles m^{-3})[a,b,c]
by Long Pathlength FT-IR Spectroscopy

Hourly Period (PDT)	Sept 11	Sept 12	Sept 13	Sept 14[d]	Sept 15	Sept 16	Sept 17[d]	Sept 18
0800-0900	BD	BD	BD	BD	BD	BD	BD	BD
0900-1000	BD	BD	BD	BD	BD	BD	BD	BD
1000-1100	BD	BD	BD	270	BD	BD	BD	BD
1100-1200	BD	BD	BD	450	≤160	BD	BD	BD
1200-1300	BD	BD	XX	540	≤250	BD	BD	BD
1300-1400	BD	BD	≤440	510	≤380	BD	130	BD
1400-1500	BD	BD	≤420	510	XX	≤200	310	BD
1500-1600	BD	XX	≤540	860	≤350	≤140	270	BD
1600-1700	BD	XX	≤470	770	≤270	BD	140	BD
1700-1800	BD	≤330	XX	350	XX	BD	BD	BD
1800-1900	BD	≤290	XX	BD	XX	BD	BD	BD
1900-2000	BD	BD	XX	BD	BD	BD	BD	BD
2000-2100	BD	BD	XX	BD	BD	BD	BD	BD
2100-2200	BD	BD	XX	BD	BD	BD	BD	BD

[a] At 23°C and 740 torr (conversion factor: 1 ppb = 40 nanomoles m^{-3}).
[b] Concentrations for periods earlier and later than the time periods shown are below detection limit (<160 nanomoles m^{-3}).
[c] BD: Below detection; XX indicates indeterminate concentration due to very high noise level in the spectra; ≤ symbol designates an upper limit estimate (dictated by the presence of significant noise in some of the spectra in the data set).
[d] Error: ±160 nanomoles m^{-3} (±4 ppb).

Appendix B

Hourly Average NH_3 Concentrations (nanomoles m^{-3})[a,b,c] by Long Pathlength FT-IR Spectroscopy

Hourly Period (PDT)	Sept 11	Sept 12	Sept 13	Sept 14	Sept 15	Sept 16	Sept 17	Sept 18	Sept 19
0000-0100		-	140	-	88	92	60	76	75
0100-0200		-	140	-	140	92	68	88	71
0200-0300		-	130	-	100	120	76	88	60
0300-0400		-	120	-	110	88	48	130	54
0400-0500		-	120	-	100	68	210	110	73
0500-0600		-	98	-	84	48	430	110	85
0800-0900	77	150	240	170	220	1260	610	110	
0900-1000	110	220	260	180	230	940	690	81	
1000-1100	110	250	420	160	250	900	1850	95	
1100-1200	89	200	1340	140	280	1330	1590	80	
1200-1300	61	610	640[d]	190	290	710	840	74	
1300-1400	69	1680	300	160	260	240	240	40	
1400-1500	100	2280	180	190	210[d]	180	140	84	
1500-1600	95	580[d]	180	150	170	130	120	120	
1600-1700	73	330[d]	160	160	170	160	140	120	
1700-1800	93	190	170[d]	200	140[d]	120	110	160	
1800-1900	110	190	XX	180	140[d]	140	84	170	
1900-2000	130	240	XX	220	160	120	92	120	
2000-2100	160	210	XX	170	190	130	140	140	
2100-2200	110	260	XX	190	92	120	130	100	
2200-2300	-	160	-	140	140	-	140	100	
2300-2400	-	140	-	120	120	-	100	100	

[a] At 23°C and 740 torr (conversion factor: 1 ppb = 40 nanomoles m^{-3}).
[b] Error: ±60 nanomoles m^{-3}; detection sensitivity = 60 nanomoles m^{-3}.
[c] Dash designates no data; XX indicates indeterminate concentrations due to very high noise levels in the spectra.
[d] A higher error limit of ±100 nanomoles m^{-3} has been estimated for these periods.

Appendix C

Average HNO_3 Concentrations (nanomoles m^{-3})[a,b,c] by Long Pathlength FT-IR Spectroscopy for the Designated Sampling Periods

Sampling Period (PDT)	Sept 11	Sept 12	Sept 13	Sept 14	Sept 15	Sept 16	Sept 17	Sept 18	Sept 19
0000-0600		-	<160	-	<160	<160	<160	<160	<160
0800-1200	<160	<160	<160	180-260	<160	<160	<160	<160	
1200-1600	<160	<160	(405)	605	(340)	(85-165)	180-220	<160	
1600-2000	<160	XX	XX	280-360	XX	<160	<160	<160	
2000-2400	<160	<160	-	<160	<160	<160	<160	<160	

[a]Dash means incomplete or no data; XX designates an indeterminate value due to the presence of excessive noise levels in a significant number of spectra in the block.

[b]See text for the method used in estimating the concentration range for a particular block.

[c]An error of ±160 ppb applies to the values or range of values for September 14 and 17; this error does not apply to the values in parentheses which were largely derived from upper limit hourly concentrations (Appendix A).

Appendix D

Average NH_3 Concentrations (nanomoles m^{-3})[a] by Long Pathlength FT-IR Spectroscopy for the Designated Sampling Periods

Sampling Period (PDT)	Sept 11	Sept 12	Sept 13	Sept 14	Sept 15	Sept 16	Sept 17	Sept 18	Sept 19
0000-0600		-	125	-	103	85	150	102	70
0800-1200	97	205	567	163	245	1110	1190	92	
1200-1600	81	1290[b]	325[b]	173	233[b]	315	335	84	
1600-2000	102	238[b]	XX	190	153[b]	135	105	143	
2000-2400	-	193	-	155	135	-	128	110	

[a]Dash means incomplete or no data; XX designates an indeterminate concentration due to the presence of excessive noise in a significant number of spectra in the block. Error = ±60 nanomoles m^{-3} unless noted otherwise.

[b]An uncertainty of ±80 nanomoles m^{-3} applies to these values.

CARB LIBRARY
08794